

# A powder-based approach to semisolid processing of metals for fabrication of die-castings and composites

R. M. K. YOUNG, T. W. CLYNE\*

*Department of Materials Science and Engineering, University of Surrey, Guildford, Surrey, UK*

A technique is presented for the generation of a globular (non-dendritic) array of solid fragments surrounded by a solute-enriched liquid. This is based on the premixing, heat treatment and consolidation of different types of powder. The resultant slurries have then been injected into a die at high velocity. The technique offers promise in terms of the versatility with which the slurry microstructure can be controlled and the soundness of the resulting die-castings has been encouraging. Among the effects investigated are the role of solute diffusion, the importance of globule size and the nature of coarsening phenomena. Experiments have also been carried out on the incorporation of ceramic fibres into the product and this appears to offer promise as a composite fabrication route. The work described here concerns only aluminium-base material alloyed with magnesium, although the principles outlined are expected to apply to many other systems.

## Nomenclature

### Parameters

$C$	composition (mass fraction)
$d$ (m)	diameter
$D$ (m <sup>2</sup> sec <sup>-1</sup> )	diffusivity
$f$	volume fraction
$k$	partition coefficient
$L$ (m)	characteristic length
$Q$ (J mol <sup>-1</sup> )	activation energy
$r$ (m)	radius
$R$ (J K <sup>-1</sup> mol <sup>-1</sup> )	gas constant
$Re$	Reynolds number
$t$ (sec)	time
$T$ (K)	temperature
$u$ (m sec <sup>-1</sup> )	fluid velocity
$We$	Weber number

$\lambda$	aspect ratio
$\mu$ (Pa sec)	dynamic viscosity
$\rho$ (kg m <sup>-3</sup> )	density
$\sigma$ (J m <sup>-2</sup> )	surface tension

### Subscripts

d	dispersoid
f	fusion point
g	globule
L	liquidus
m	matrix
r	relaxation
s	solid
S	solidus
*	solid/liquid interface

## 1. Introduction

### 1.1. Concepts and objectives

The processing of metals while in the form of a mixture of liquid and solid phases is of considerable current interest. This can to some extent be traced to the work of Flemings and co-workers [1-4] in the 1970s, when the term "rheocasting" was coined for a technique in which local shear forces are maintained within a body of solidifying liquid. This can continuously disrupt the growing dendrite array to such an extent that the resultant structure is composed of isolated "globules" of primary solid (surrounded by the solute-rich material corresponding to the residual liquid), rather than the normal interlocking network of a branched dendritic morphology.

Characterization of the rheological behaviour of such a material when semisolid continues to receive considerable attention [5-8]. The globular material will flow as a rather viscous slurry under the influence of

appropriate shear stresses. This can be exploited with a volume fraction of solid around, say, 50%, for which the corresponding normal dendritic material would probably remain rigid until a stress were reached at which gross defects would be generated. This feature offers potential for processing techniques in which a body of semisolid globular material is made to undergo a selected change of shape; this is particularly attractive in view of the fact that the solute distribution can be tailored so that the globular state is recreated from the fully solidified structure by simply reheating to an appropriate temperature.

One of the most promising areas of application is in pressure die-casting [4, 7, 9-11], in which the charge is injected at high velocity (primarily to inhibit premature solidification). As a result of the low viscosity of liquid metals (typically about the same as that of water), such material enters the die cavity in a highly turbulent manner, frequently involving break-up of the stream

\*Present address: Department of Metallurgy and Materials Science, Pembroke Street, Cambridge, UK.

and atomization [9, 10]. This results in entrainment of air, causing internal porosity and a poor surface finish, problems which have effectively limited the market for die-castings. Replacement of the liquid charge by a semisolid slurry can result in progressive, controlled filling of the die. Among other important advantages offered by the slurry route are reduced thermal shock to the die [4, 7] and a smaller contraction (contributing to the reduction in porosity). Such points have been recognized for some time and have been summarized by Brook [9].

## 1.2. Rheology

It is well established that the viscosity of globular metallic slurries is dependent on the strain rate; i.e. they are non-Newtonian fluids. Fig. 1 shows schematic variations of shear stress as a function of the strain rate, for different categories of fluid. (The dynamic viscosity is given by the gradient of such a plot.) In addition to a possible dependence on strain rate, the viscosity of a fluid may decrease (thixotropic) or increase (rheopectic) with time under steady conditions [12], as a result of microstructural changes. The term "thixocasting" has been rather loosely applied to die injection of a metallic slurry (formed by reheating a rheocast structure), the terminology arising from the idea of the slurry exhibiting a decrease in viscosity on processing. This is somewhat misleading, as there is no time dependence to the viscosity during the process (which is a very rapid one), but rather a sharp drop as the high shear stresses are generated\*. It is clear from Fig. 1 that these metallic slurries are more properly regarded as pseudoplastic Bingham fluids.

An attempt at (semi-quantitative) correlation of these features with the operating conditions is shown in Fig. 2. The applied (inertial) force is considered as a ratio to the viscous (damping) force and as a ratio to the surface tension force. These two ratios correspond to the Reynolds number,  $Re$ , and the Weber number,  $We$ , respectively:

$$Re = \frac{Luq}{\mu} \quad (1)$$

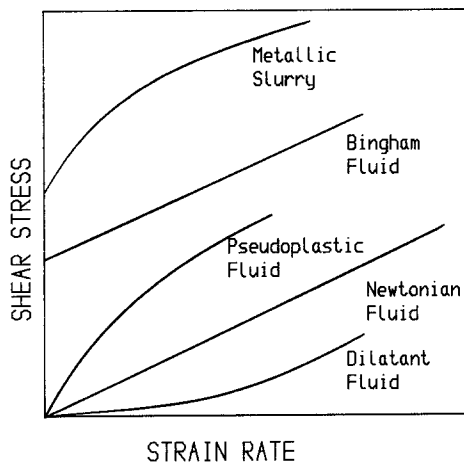


Figure 1 Schematic plots of shear stress against shear strain rate for different types of fluid.

\*A time dependence does, however, tend to arise during rheocasting, although this is often manifest as an increase in viscosity and indiscriminate use of the word "thixotropy" in this context can cause further confusion. In fact usage of the word to describe various non-Newtonian effects has expanded to the point where its definition may be considered to be in some doubt.

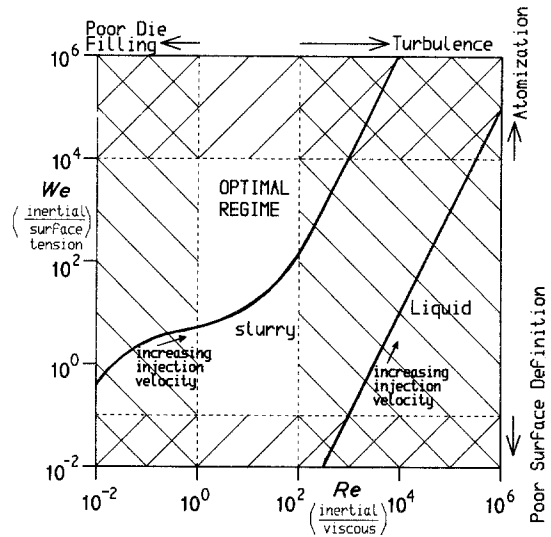


Figure 2 Illustrative plot showing the variation of parameters characterizing the surface tension ( $We$ ) and viscous drag ( $Re$ ) with changing fluid velocity, for a typical metallic liquid and semisolid (globular) slurry. Also shown are approximate regimes of these parameters for which various problems associated with die casting might occur.

$$We = \frac{Lu^2 \rho}{\sigma} \quad (2)$$

where  $L$  is a characteristic length,  $u$  is the fluid velocity,  $\rho$  is the fluid density,  $\mu$  is the dynamic viscosity and  $\sigma$  is the surface tension. An increase in applied stress during injection will raise both of these numbers. For a Newtonian fluid, these increases will be solely due to the higher value of  $u$  and the operating point on this plot will move in a linear fashion, with a gradient of 2. The problem caused by low viscosity is manifest as a high  $Re$  for all practicable injection velocities (which might range upwards from several  $\text{m sec}^{-1}$ ).

For a non-Newtonian fluid, on the other hand, the effect of an increase in injection velocity is compounded by the associated change in viscosity. Unfortunately, the strain rate regime of interest is one in which it is difficult to measure the viscosity and the exact position of the curve for the slurry is open to speculation. Viscosity measurements have been made [5, 13, 14] for shear strain rates up to several hundred  $\text{sec}^{-1}$ , but die injection might involve a figure of perhaps  $10^3$  to  $10^4 \text{ sec}^{-1}$ . In view of this, one might justifiably refer to an "impact viscosity" which, while probably amenable to extrapolative estimation, should be identified as differing from that obtained by conventional measurement. In any event, there is no doubt that the curve is shifted to lower Reynolds number relative to that of the liquid and the existence of an optimal fluid dynamics operating regime (which is approached by moving in this direction) seems clear.

## 1.3. Microstructure

Clearly, one expects the viscosity to increase with increasing fraction of solid; Joly and Mehrabian [13] have highlighted the role of entrapped liquid in tending to raise the viscosity by increasing the effective value of

$f_s$  (the fraction of solid). As one objective is normally to achieve a high true fraction solid while not exceeding an upper limit on the viscosity, such entrapment is generally undesirable. It should also be recognized that globules in a metallic slurry tend to interact with each other and thus exhibit higher viscosities (relative to the base liquid) than suspensions of non-interacting spheres at the same fraction solid [13]. Furthermore, assemblies of metallic globules are prone to agglomerate by contact welding, raising the effective fraction of solid and thus increasing the viscosity. This is progressive and the time dependence can give rise to rheopectic behaviour during prolonged semisolid processing.

There have also been suggestions [13] that viscosity rises with increasing globule size, possibly as a result of the greater momentum transfer during collisions [15]. However, it should be noted that experimental support for this (from rheocasting data) is inconclusive in that, although low viscosity and fine globule size tend to occur in tandem, the latter could be a side-effect of the higher shearing forces, which are acting to reduce the viscosity primarily by preventing agglomeration (liquid entrapment) and by minimizing globule interactions. Certainly, theoretical analysis [16] suggests no such dependence on absolute size *per se*, although aggregation, size distribution and particle aspect ratio are all predicted to have significant effects, at least for Newtonian suspensions. Such treatments do not, however, take account of geometrical constraints, such as the size of an orifice the slurry is to pass through, or the dimensions of a re-entrant it is to penetrate. Globule size will probably be important if it is not very much smaller than the scale of such environments and this could be a point of practical significance.

#### 1.4. Diffusional effects

Solute redistribution occurs both as solid/liquid partitioning and as back-diffusion in the solid. (The composition is normally uniform at all times in all of the liquid.) This can affect the slurry behaviour via an influence on the fraction of solid and the globule characteristics. This has been emphasized previously [17, 18] and, indeed, a process has been proposed [19] in which solidification is controlled entirely by back-diffusion. This affects the fraction of solid (after the setting up of interfacial equilibrium at a given temperature) by tending to lower (for  $k < 1$ ) the interfacial solid composition and thus to provoke further solidification to maintain equilibrium at the interface.

It has been common [1, 13, 20] to assume that, for a binary alloy system with linear liquidus and solidus lines, the fraction of solid ( $f_s$ ) during slurry production and processing can be related to the temperature via the Scheil equation (based on negligible back-diffusion)

$$f_s = 1 - \left( \frac{T_f - T}{T_f - T_L} \right)^{1/(k-1)} \quad (3)$$

where  $k$  is the partition coefficient,  $T_f$  is the solvent fusion point and  $T_L$  is the liquidus temperature. Although this constitutes a good approximation for normal solidification with a substitutional solute, deviations are expected here for at least two reasons. Firstly, the Scheil assumption of no back-diffusion is valid over

a range of conditions only because slow cooling (i.e. a greater time for diffusion) normally leads to coarser spacings (i.e. greater diffusion distances): the correlation between cooling rate and spacing is abrogated for slurries, when an extended period in the semisolid regime can occur in combination with a relatively fine globule size. Secondly, the Scheil assumption of a plate-like morphology is clearly invalid for slurries, where a spherically symmetrical model would be more appropriate.

Both of these factors tend to enhance the significance of back-diffusion. Use of the equation of Brody and Flemings [21] leads to inconsistencies for extensive back-diffusion and, although the equation of Clyne and Kurz [22] behaves correctly in this limit, it is generally preferable to develop a numerical model, allowing freedom to specify geometry, thermal history and material properties. A number of workers have recognized this, although there is still a shortage of good theoretical and experimental data in the literature.

#### 1.5. Production

The "standard" methods of producing a globular metallic slurry remain centred around the idea of introducing mechanical shear stresses during solidification, usually by means of some form of rotary motion. The process has been extensively analysed [13, 20, 23, 24] and considerable engineering expertise has been brought to bear on the problem. However, although suitable globular microstructures can be produced in this way (an example is shown in Fig. 3), the process is subject to severe theoretical limitations and technical difficulties. In the former category come the constraints on production rate imposed by the combined requirements of heat extraction and local shear stress, while the interrelationships between cooling rate, globule size and (effective) fraction solid mean that freedom to tailor the microstructure is limited. Among the many technical problems are those arising from an inherent instability in process control, caused by the tendency for an increase in flow rate out of the rheocaster to result in reduced slurry viscosity (encouraging more rapid flow). Difficulties such as these are recognized by all who have been involved with the process, but, despite considerable interest, very little has emerged so far into the open literature in the way of alternative production routes.

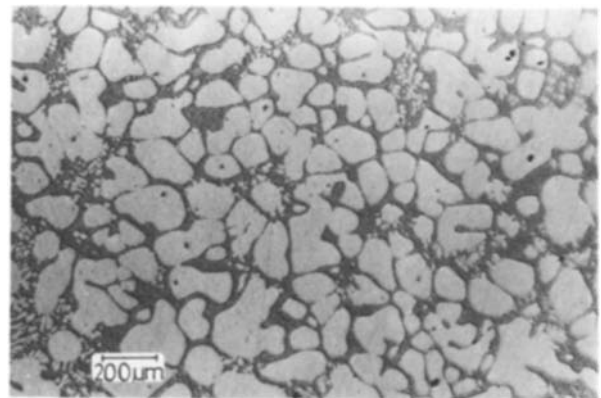


Figure 3 Typical rheocast structure, in this case for an Al-Cu alloy.

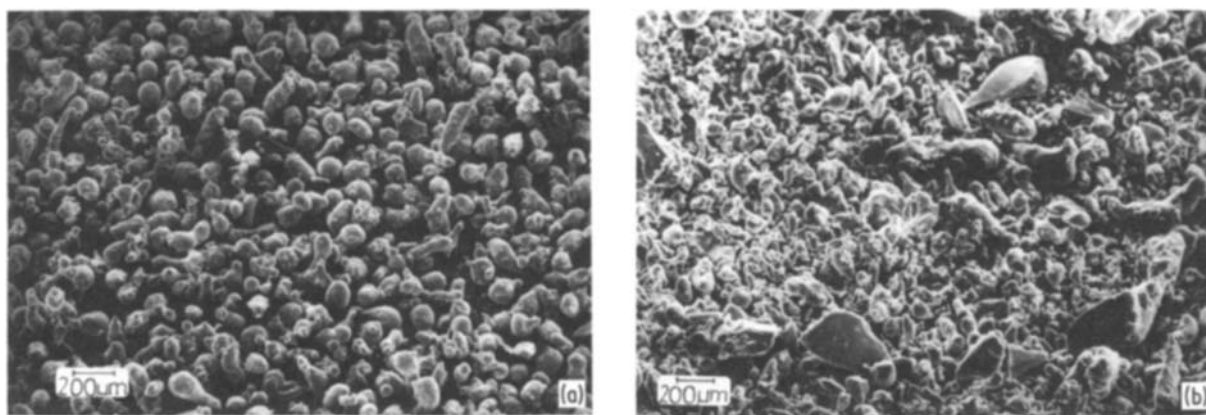


Figure 4 Micrographs of (a) an aluminium powder and (b) the corresponding mixture with the Al-Mg powder (billet 1).

## 2. Powder processing

### 2.1. Fabrication procedure

A route has been developed for fabrication of metallic slurries, based on the premixing and compaction of different powders. The technique has been termed consolidation of mixed powders as synthetic slurry (COMPASS). The consolidation step involves melting some of the material and compacting under pressure to eliminate porosity. A heat treatment stage can also be incorporated in order to generate the desired solute distribution. It would normally be considered desirable for the particles which are to remain solid to have an approximately spherical morphology. Within the limits of powder availability and subject to the microstructural changes taking place during consolidation, there is complete freedom to specify the size and volume fraction of the globules and the compositions of the globular and surrounding material.

Initial mixing is carried out in a liquid suspension medium. The constituent powders, together with any additional material such as fibres (see Section 4), are dispersed (in the selected proportion) in a suitable liquid (industrial methylated spirits was used in the present study) to form a suspension volume fraction of the order of 20%. This is then agitated (a standard domestic liquidizer was employed) for a few minutes and allowed to settle. Excess liquid is decanted off and the residue dried by gentle heating and exposure to vacuum. Much of the work reported here is based on “globule powders” of unalloyed aluminium, mixed with “matrix powders” of Al-50 wt % Mg, the former being approximately spherical (depending on size and method of production) and the latter exhibiting a faceted morphology. Fig. 4 compares the appearance of one of the aluminium powders used with that of the corresponding mixture.

The powder residue from the above operation is first cold-pressed to give a “green” compact. This is then heated (under argon) into the semisolid regime, decanted into a die held at about 300°C and immediately subjected to a directional pressure of about 30 MPa for a couple of minutes or so. This produces a sound, cylindrical billet 60 mm diameter, with a length of around 75 mm, which could form the charge for a die-injection operation. Heating of the green compact was carried out in a graphite crucible subjected to r.f. heating and the necessity of avoiding

excessive temperature differences within the melting mixture restricted heating rates to about 0.5 to 1 K sec<sup>-1</sup>. As a result of these features, the minimum total residence time in the semisolid regime during billet fabrication was typically of the order of several minutes. In addition, a similar (perhaps slightly shorter) period would be necessary during subsequent reheating and injection into the die (see Section 5).

### 2.2. Specimen characterization

In an attempt to investigate a range of slurry structures, various sizes and morphologies of globule powder were used, whereas a single grade of Al-50 wt % Mg material was employed for the matrix material (which melts during processing). In addition, some experiments were carried out with unmixed alloy powders. Table I gives details of the powdered combinations referred to in this paper. (The parameter  $\lambda$  is a mean aspect ratio.) Table II sets out subsequent thermal histories experienced by these specimens. (The  $f_s$  ranges given are calculated values — see Section 3.1.) This is a small subset of the complete experimental program.

Most of the specimens prepared for optical microscopy were viewed in polarized light after the application of an anodizing treatment, which reveals globule orientation information. Anodizing was carried out for about 40 sec in 5% fluoroboric acid, using a potential designed to give a high current density of the order of 300 A m<sup>-2</sup>). Specimens for energy dispersive X-ray microanalysis were polished flat and analysed with an electron accelerating voltage of 10 kV. Die castings were subjected to several types of examination for soundness, including X-ray radiography.

### 2.3. Progress of consolidation

The green compact was typically about 70% dense; Fig. 5a shows an illustrative structure. After heating to the semisolid regime, the magnesium-rich powder melts and surface tension forces drive the liquid to fill much of the interglobular space. It is apparent in Fig. 5b that melting of the solute-rich material is rapidly followed by surface liquation of the aluminium particles where there is contact with this liquid. This takes place as the system moves towards interfacial equilibrium (see next section). Hot pressing completes the envelopment of the globules by solute-rich liquid, leading to very low porosity levels in the

TABLE I Constitution of billets

Billet number	Globule powder				Matrix powder				Dispersoid			
	$C_g$ (wt % Mg)	$d$ ( $\mu\text{m}$ )	$\lambda$	$f_g$ (%)	$C_m$ (wt % Mg)	$d$ ( $\mu\text{m}$ )	$\lambda$	$f_m$ (%)	Type	$d$ ( $\mu\text{m}$ )	$\lambda$	$f_d$ (%)
1	0	90	1.2	80	50	150	5	20	—	—	—	—
2	0	90	1.2	80	50	150	5	20	—	—	—	—
3	0	90	1.2	80	50	150	5	20	—	—	—	—
4	0	90	1.2	80	50	150	5	20	—	—	—	—
5	0	40	1.5	80	50	150	5	20	—	—	—	—
6	0	40	1.5	80	50	150	5	20	—	—	—	—
7	10	40	1	100	—	—	—	—	—	—	—	—
8	10	40	1	100	—	—	—	—	—	—	—	—
9	0	40	1.5	72	50	150	5	18	Al <sub>2</sub> O <sub>3</sub> fibre	3	150	10
10	0	40	1.5	72	50	150	5	18	Al <sub>2</sub> O <sub>3</sub> fibre	3	150	10
11	0	90	1.2	60	50	150	5	40	—	—	—	—
12	0	10	1.3	80	50	150	5	20	—	—	—	—
13	0	10	1.3	80	50	150	5	20	—	—	—	—

final billet. A typical microstructure is shown in Fig. 6a. Thermal control is important and overheating can lead to partially dendritic structures of the type shown in Fig. 6b. (Globule size also plays an important role in this, as explained in Section 3.1). Certain billets were then subjected to further heat treatments prior to die casting. Details of the injection of the slurry into the die are covered in Section 5.

### 3. Microstructural stability

#### 3.1. Solute diffusion effects

An idealized version of the relevant portion of the Al–Mg phase diagram is shown in Fig. 7, on which the liquidus and solidus compositions at 750 K are indicated. A finite difference model was set up to describe the back-diffusion after interfacial equilibrium is established. The initial state is taken as liquid with a uniform composition of  $C_L$  (liquidus for temperature concerned) surrounding a solid sphere with an unchanged solute level in the interior, but a surface composition that had been raised to the solidus,  $C_S$ . Neglect of the transient between melting of the matrix powder and the attainment of this state is easily justified in terms of solute diffusion rates in the liquid, but takes no account of heat flow through the billet section for cases where this transient involves melting a

substantial amount of globule powder. It can be shown that, partly as a result of the high thermal diffusivity of aluminium, this is not expected to delay the attainment of interfacial equilibrium for more than a short period (perhaps a minute or so). This delay might, however, be significant for fine powders. The system is composed of a solid sphere surrounded by a spherical shell of liquid. (A more geometrically accurate model would treat the liquid as something like a hollow tetrakaidecahedron, but the mathematical complexity introduced in this way is difficult to justify in view of other approximations implicit in the analysis.)

The appropriate form of the diffusion equation describing solute redistribution in the solid is:

$$\frac{\partial C}{\partial t} = D_s \left( \frac{\partial^2 D_s}{\partial r^2} + \frac{2}{r} \frac{\partial C}{\partial r} \right) \quad (4)$$

assuming spherical symmetry and neglecting any composition dependence of the solute diffusivity,  $D_s$ . This is solved under the following boundary conditions:

$$C = C_g \quad \text{for } r < r_*, \quad t = 0 \quad (5)$$

$$C = C_L \quad \text{for } r > r_*, \quad t \geq 0 \quad (6)$$

$$C = C_S \quad \text{for } r = r_*, \quad t \geq 0 \quad (7)$$

TABLE II Thermal histories

Billet number	Hot pressing				Heat treatment				Die injection			
	$T$	$t$	$f_s$ (%)		$T$	$t$	$f_s$ (%)		$T$	$t$	$f_s$ (%)	
	(K)	(sec)	$t = 0$	$t$	(K)	(sec)	$t = 0$	$t$	(K)	(sec)	$t = 0$	$t$
1	823	250	44	72	—	—	—	—	—	—	—	—
2	—	—	—	—	833	50	82	74	—	—	—	—
3	823	250	44	72	—	—	—	—	—	—	—	—
4	860	250	16	29	—	—	—	—	—	—	—	—
5	823	250	44	85	—	—	—	—	850	200	60	50
6	823	250	44	85	837	7200	75	69	—	—	—	—
7	823	250	85	85	—	—	—	—	850	200	60	50
8	823	250	85	85	837	7200	68	68	—	—	—	—
9	—	—	—	—	823	250	44	85	—	—	—	—
10	823	250	44	85	—	—	—	—	865	200	40	25
11	750	200	35	45	—	—	—	—	750	2000	45	55
12	—	—	—	—	823	250	60	85	—	—	—	—
13	823	250	60	85	—	—	—	—	850	200	55	50

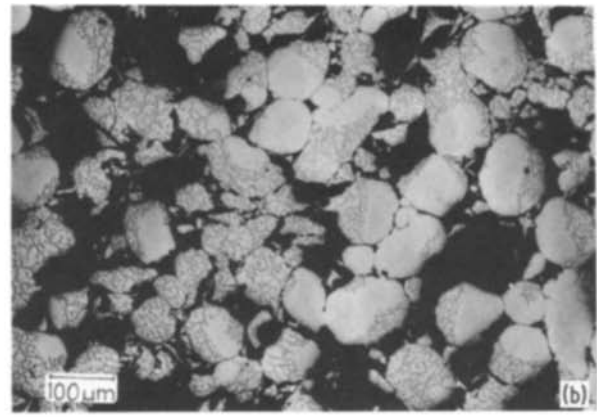
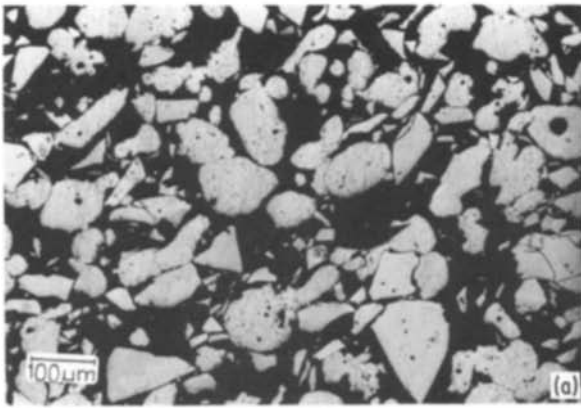


Figure 5 Optical micrographs of billet 2 (a) after cold compaction, and (b) after subsequent heating to 833 K (without hot-pressing).

$$r_* = r_g f_g^{-1/3} (C_L - C_g)^{-1/3} \times [C_L - C_g f_g - C_m (1 - f_g)]^{1/3} \quad \text{for } t = 0 \quad (8)$$

$$\frac{\partial r_*}{\partial t} = \frac{D_s}{(C_L - C_s)} \frac{\partial C}{\partial r} \Big|_{r_*} \quad (9)$$

where  $r_g$ ,  $C_g$  and  $f_g$  are the initial radius ( $= d_g/2$ ), composition and volume fraction of the globule material,  $C_m$  is the initial composition of the matrix powder and  $r_*$  is the instantaneous radius of the solid sphere. It is assumed that powder compositions and holding temperature will have been chosen such that attainment of interfacial equilibrium will involve melting of the matrix powder, plus some of the globule powder. Any volume change associated with freezing/melting is neglected. A finite difference reduction formula derived from truncated Taylor series expansions was used and an explicit method employed to obtain the solutions. The system was assumed isothermal, with a diffusivity given by:

$$D_s = D_0 \exp(-Q/RT) \quad (10)$$

where  $D_0$  and  $Q$  for the Al-Mg system have approximate values of  $0.1 \text{ m}^2 \text{ sec}^{-1}$  and  $175 \text{ kJ mol}^{-1}$  [25]. Most of the computations were carried out with 100 or 200 volume elements spanning the domain. Fig. 8 shows a typical radial concentration profile after a specified time for a given set of conditions.

This model was used to explore the rate at which

different systems would approach the fully equilibrium condition (corresponding to a uniform composition in the solid phase) for which the solid fraction would be that given by the lever rule:

$$f_s = \left( \frac{1}{1-k} \right) \left( \frac{T_L - T}{T_f - T} \right) \quad (11)$$

As expected, the predictions are sensitive to both temperature and system dimensions. Fig. 9 shows  $f_s$  as a function of time for three initial values of the globule diameter, at a temperature of 823 K (550°C). It should be noted that, for fine powders ( $d \leq 50 \mu\text{m}$ ), the rise in  $f_s$  from the value corresponding to interfacial equilibrium ( $t = 0$ ) towards that of the final state takes place very rapidly. The back-diffusion causing this will start to occur during the (neglected) transient associated with melting of some of the globule material (while interfacial equilibrium is being set up). The upshot of this is that the fraction of solid will probably not fall as far as the predicted minimum ( $t = 0$ ) value with fine powders, which might thus be expected to be less susceptible to the effects of accidental overheating than coarser mixtures.

If a value for the relaxation time,  $t_r$ , defined in terms of a 90% approach to the lever rule state

$$t = t_r \quad \text{at } f_s = f_s^r = 0.9 f_s^\infty + 0.1 f_s^0 \quad (12)$$

is extracted for different cases, then a plot such as that of Fig. 10 may be constructed to highlight the effect of size and temperature over the regime of interest. In

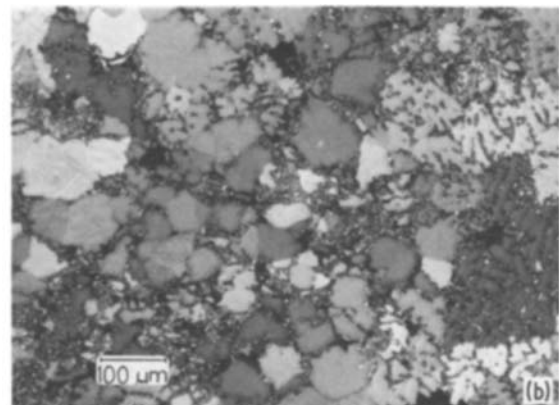
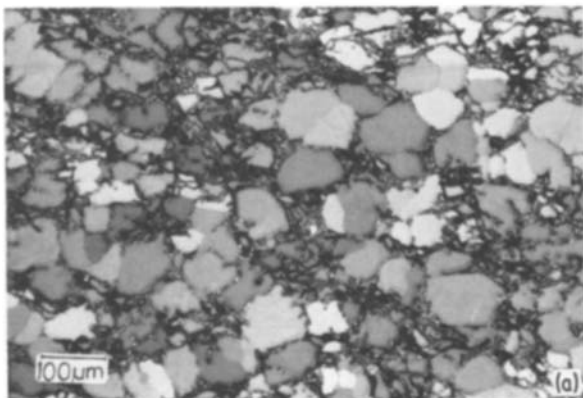


Figure 6 Optical micrographs of hot-pressed billets: (a) billet 3, showing a normal COMPASS structure, and (b) billet 4, showing the effect of overheating.

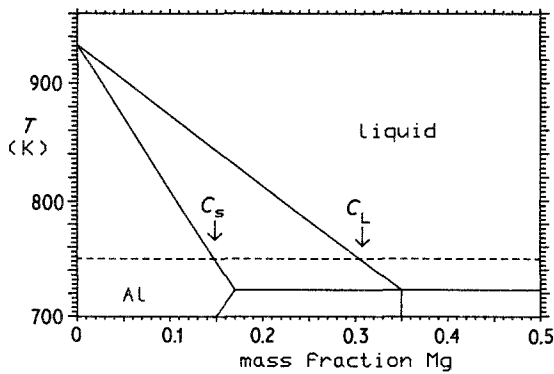


Figure 7 A simplified version of the aluminium-rich half of the Al-Mg phase diagram, showing the liquidus and solidus compositions at 750 K.

general, at temperatures above about 800 K, it is expected that lever rule conditions will be approached within the minimum processing time ( $\approx 5$  to 10 min) for fine powder ( $d \leq 70 \mu\text{m}$ ) and only with coarse material ( $d \geq 150 \mu\text{m}$ ) will prolonged heat treatment be necessary to attain this state. However, these figures would be different for the lower processing temperatures ( $\approx 750 \text{ K}$ ) which might be appropriate for more solute-enriched material, and in general it is clear that the sensitivity to  $T$  and  $d$  is such that most cases require individual computation. (Nevertheless, an obvious conclusion is that use of the Scheil equation is unjustified under most conditions.) In fact, these characteristics carry a convenient implication in terms of the processing of fine powders in that the volume fraction of solid (at a given temperature) can be accurately preselected simply by controlling the initial powder volume ratio and there need then be no concern about rigorous programming of the thermal history. Coarser material, on the other hand, might experience progressive changes in  $f_s$  during prolonged isothermal treatment.

Experimental monitoring of the diffusional effects was undertaken via electron probe microanalysis. The approach adopted was to use the minimum composition detected to characterize progression of the back-diffusion. Measurements were taken near the centre of globules which appeared to have had a diameter close to the median for the specimen. This was repeated several times for different globules in an

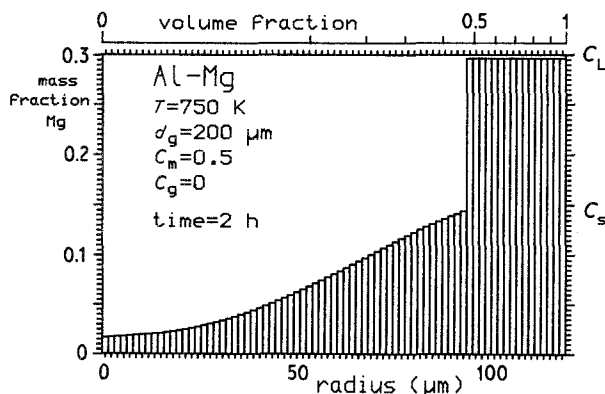


Figure 8 Theoretical radial concentration profile for the case shown, 2 h after the attainment of interfacial equilibrium, indicating the volume element width for this particular computation.

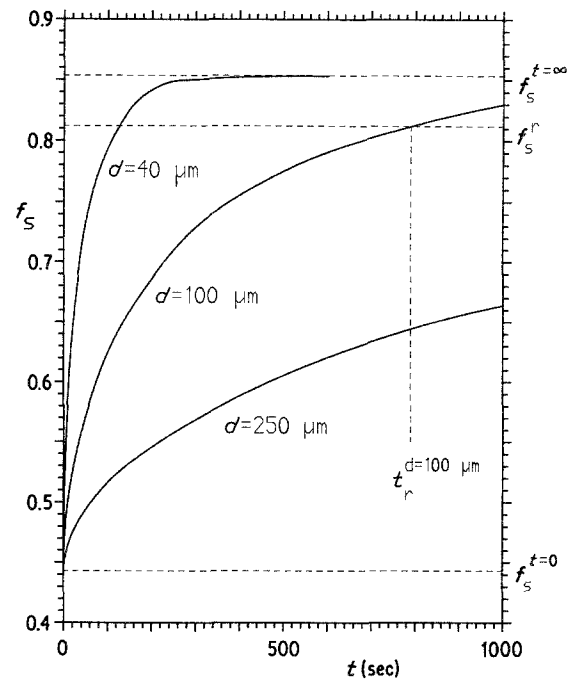


Figure 9 Predicted changes of fraction solid with time as a result of back-diffusion. The curves are for the powder compositions and proportion shown, with three different values for the initial (premelting) diameter of the globule particles. The construction for estimating the relaxation time  $t_r$  is shown for the  $100 \mu\text{m}$  case.

attempt to minimize errors arising from uncertainties about the sectioning geometry. Fig. 11 shows a typical microprobe trace, superimposed on a micrograph with the corresponding scan line marked. As a general verification of the validity of the back-diffusion model, Fig. 12 compares theoretical curves for the changing magnitude of  $C_{\text{min}}$  (the centre-point composition) with a number of experimental values (each of which is derived from several scans), referring to globules in two size ranges which had undergone specific heat treatments.

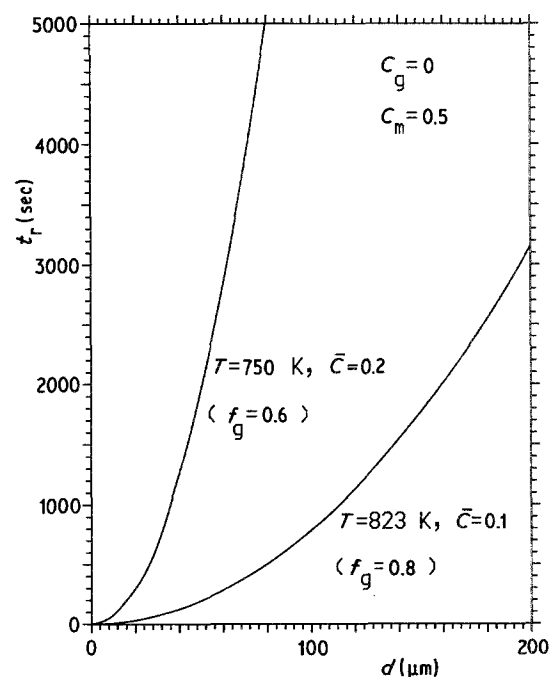


Figure 10 Predicted dependence of relaxation time on original powder diameter for two holding temperatures.



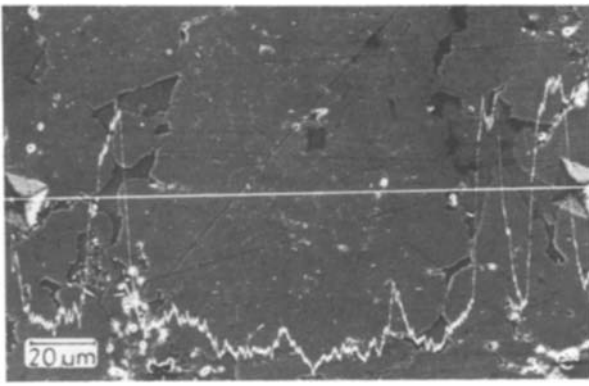


Figure 11 Typical microprobe trace across the centre of a globule (from billet 3).

### 3.2. Coarsening effects

The stability of the globule array in the semisolid regime was investigated for a range of conditions. In addition to the effect of back-diffusion, there is obviously a driving force for reduction of interfacial area and consequently a tendency for agglomeration and liquid entrapment to take place. This is, of course, a field which has been extensively investigated in sintering studies [26–31]: there is not, however, a vast amount of information relating to the high fractions of liquid ( $\approx 30$  to  $60\%$ ) which concern us here, although the work of Voorhees and Glicksman [28] (on changes in size distribution over a wide range of phase proportions) is of relevance.

In general, it was found that the globule structure tended to remain morphologically stable over the timescale for which the billets were in the semisolid regime during normal processing ( $\leq 15$  min). For example, Fig. 13 compares original globule appearance with the hot-pressed and die-cast structures for a

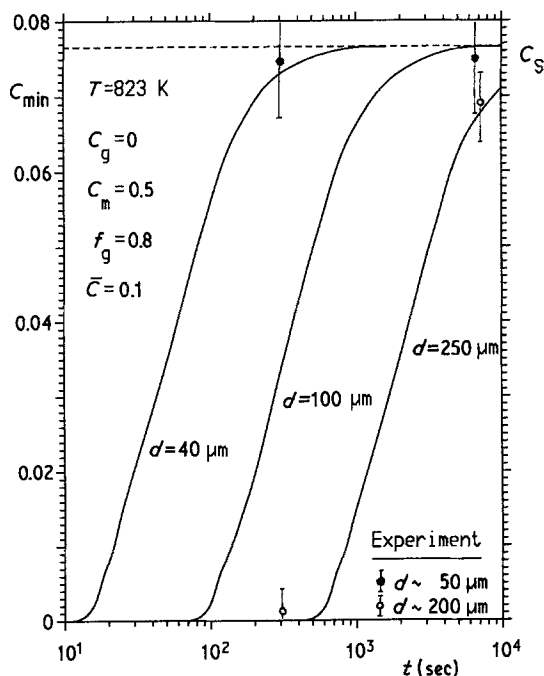


Figure 12 Comparison between the predicted curves for three original globule sizes, giving the variation of  $C_{\min}$  (centre-point composition) as a function of holding time at 823 K, and experimental points corresponding to specific times at around this temperature.

relatively fine powder exhibiting a wide size distribution ( $\approx 10$  to  $75 \mu\text{m}$ ), for which coarsening effects might have been expected to be most pronounced. It is clear that dramatic changes in the globule size distribution have not taken place. However, extended treatments do have significant effects. For example, Fig. 14 shows material from the same mixture after being held in the semisolid regime for a period of 2 h. Although some increase in mean globule size is apparent, it may be noted that the rounded morphology is maintained, and isolation of liquid pockets has not occurred to any great extent. Comparison with theory, such as classical Lifshitz and Slyozov [32] and Wagner [33] treatment of Ostwald ripening, would require more systematic data, but it seems likely that particle agglomeration and coalescence is playing a significant role in the overall coarsening behaviour in the present case.

Rather more liquid entrapment arose in some of the experiments with alloy powders. For example, some work was done using gas-atomized Al–10 wt % Mg powder which had undergone fairly rapid solidification. The internal structure of this material, shown in Fig. 15a, is composed of fine dendrites (arm spacing  $\approx 0.5 \mu\text{m}$ ). The magnesium-rich interdendritic material melts on reheating and the very short diffusion distances ensure that the fraction of solid immediately approaches that dictated by the lever rule. Much of the liquid tends to find its way to the interglobular interstices, so that it is possible to produce a suitable slurry by heating such powder without any mixing stage. However, although this is an attractive method, it can be seen in Fig. 15b that a significant amount of liquid tends to collect in pockets within the original spheres and this entrapment is probably undesirable for reasons outlined earlier. Further work is needed to clarify the significance of this effect in practical terms. It would appear from Fig. 15c that some of the entrapped liquid finds its way to the interglobular regions during extended heat treatment, although this is accompanied by considerable overall coarsening.

### 4. Composite fabrication

Discontinuous fibres, or other dispersoids, are easily incorporated at the wet blending stage and a number of such additions have been made. Some of these, particularly fibrous materials, often show a tendency to agglomerate, but it is usually possible to counter this by powder grade selection, by sizing and screening of the dispersoid and by control of the blending conditions. Fig. 16a shows a typical blended mixture, containing in this case an aluminium globule powder, an Al–50 wt % Mg matrix powder and a fine  $\delta$ -alumina fibre. (The fibre employed in the work described here was the ICI “Saffil” product. The use of this in metal matrix composites is described by Clyne *et al.* [34].) A feature apparent here is that the fibres, which were first milled and sized to an average length of around  $500 \mu\text{m}$ , have not suffered catastrophic damage during the blending, although the mean aspect ratio has dropped somewhat.

However, during subsequent billet production,



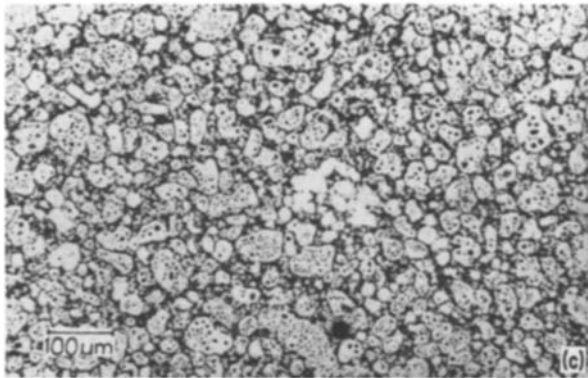
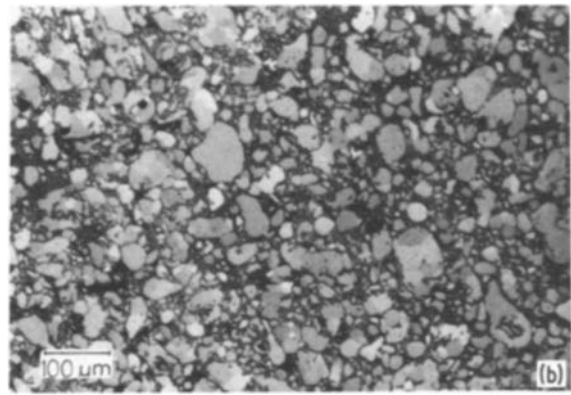
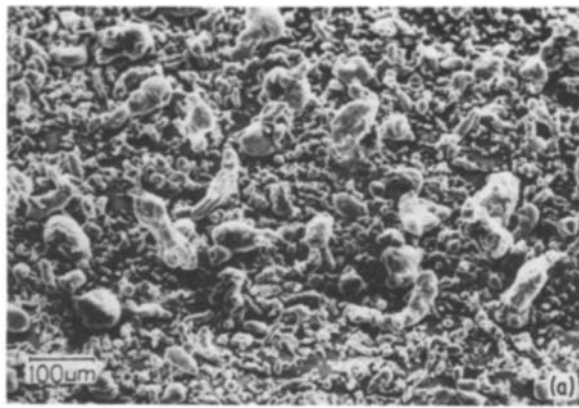


Figure 13 (a) Scanning electron micrograph of one of the globule powders used, (b) optical micrograph of a hot-pressed billet subsequently produced (billet 5), and (c) optical micrograph of final die-casting obtained from billet 5.

there is a tendency for considerable fibre fracture to occur. This takes place primarily during the cold compaction process. (It may be noted that this stage is probably not essential, and was incorporated in the present work primarily because of difficulties in fitting enough of the uncompacted semisolid mixture to form a single die-casting charge into the hot die). Fig. 16b shows the surface of a cold-pressed piece that had been heated to the semisolid regime. The fibre aspect ratio has now been considerably reduced. In any event, it proved possible to produce composite billets in which the fibres were uniformly distributed and well bonded to the surrounding metal, as shown in Fig. 16c. It may be noted that, although regions of slight fibre depletion or accumulation sometimes appeared in the billets, such inhomogeneities tended to be eliminated during the die-injection process (see next section).

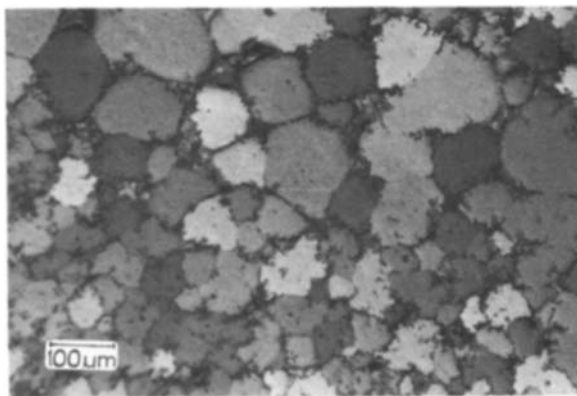


Figure 14 Optical micrograph of billet 6, which had been heat treated for 2 h at 837 K.

## 5. Die injection

Billets produced by the methods described were preheated to selected temperatures in the semisolid regime and injected\* into a die in the form of an integral web and arm of a bicycle pedal crank. The die-casting machine was a "RedRing" model. The operation was carried out with ram velocities of the order of  $3 \text{ m sec}^{-1}$ . An early pressure intensification stage was implemented (aimed at facilitating gate entry), which raised the pressure in the hydraulic system to about 30 MPa. The shot sleeve was a cylinder of 60 mm diameter, while the ingate cross-sectional area was about  $200 \text{ mm}^2$ , implying a gate entry velocity of about  $45 \text{ m sec}^{-1}$ . A typical strain rate on die entry (averaged over the gate section) would thus be of the order of  $10^3 \text{ sec}^{-1}$ . The die temperature was maintained at about  $280^\circ \text{C}$  by passing heated oil through channels in selected locations.

A die-cast microstructure is shown in Fig. 17, together with a view of the surface finish typically obtained. In general, by selection of a suitable charge temperature (and thus fraction of solid), it is possible to obtain sound castings with a globular slurry, although it should be emphasized that the gating design is not one which has been optimized for slurry casting. (Such optimization would cater for the reduced capacity for converging streams to fuse successfully, when compared with a fully liquid charge.)

One phenomenon that is noticeably characteristic of slurry die casting is enhancement of fraction liquid in certain locations near the casting surface, generating a form of solute macrosegregation. This can lead to microstructures of the type shown in Fig. 18. It may be noted that a similar type of macrosegregation (solute enrichment near heat-extracting surfaces) is frequently observed in conventional casting [35, 36] (although it is rarely pronounced in die-casting). The mechanism in such cases involves interdendritic fluid flow, primarily as a result of the volume contraction on freezing. In slurry injection, however, the mechanism is different, although it has not yet been identified in detail. The most likely explanations are either that the liquid is being squeezed through an assembly of

\*The die-casting operations were carried out at Fulmer Research Laboratories.

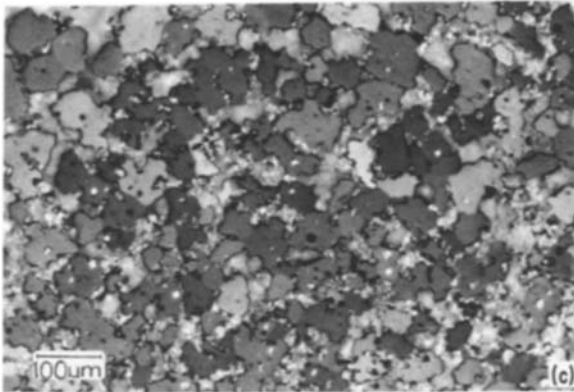
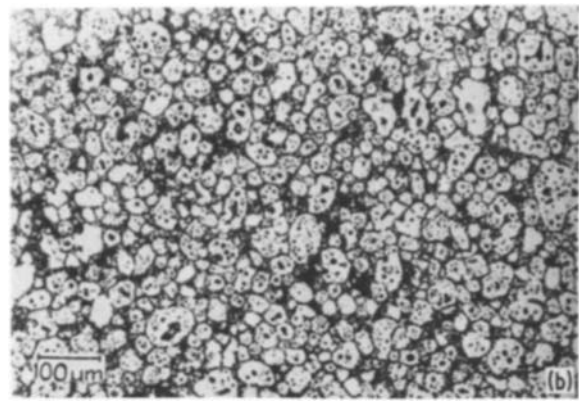
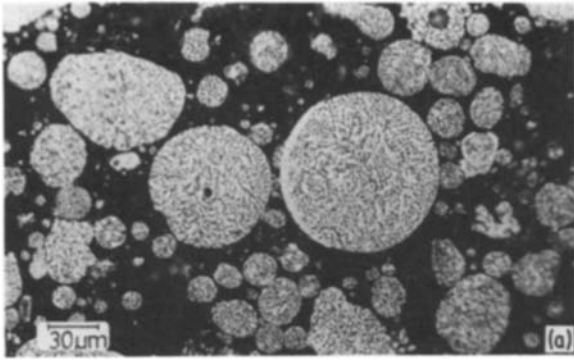


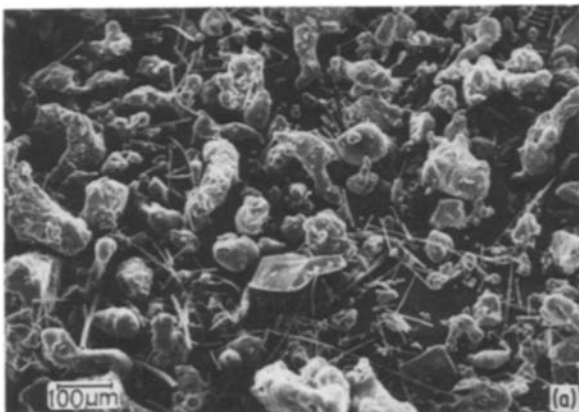
*Figure 15* Optical micrographs showing structures based on a single grade of Al-10 wt % Mg powder, (a) as-received (gas atomized), (b) die-cast (billet 7), and (c) heat treated for 2 h at 837 K (billet 8).

globules rendered relatively immobile near the end of die-filling by interglobular welding, or that the sharp gradient of strain rate near the periphery of the flow cross-section has driven globules towards the centre, generating a type of central “plug flow” surrounded by a globule-depleted annulus accomodating most of

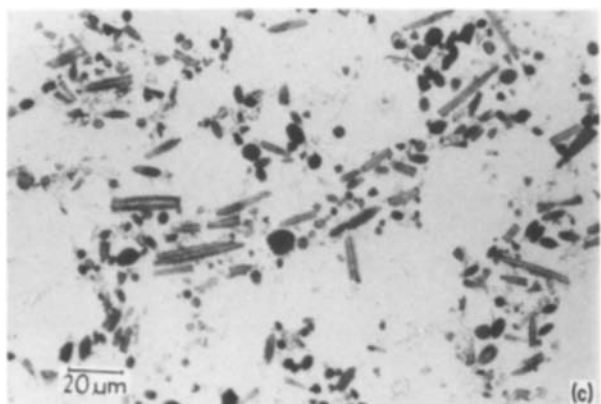
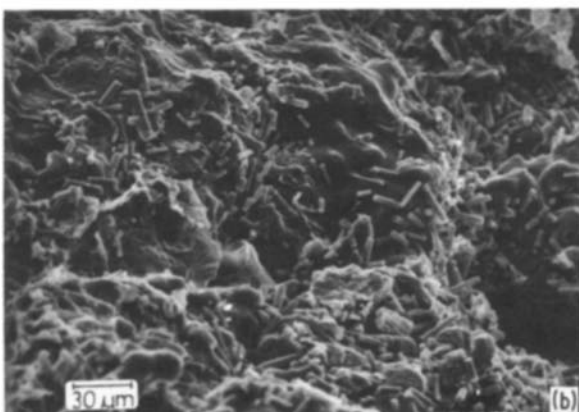
the shear strain. It is possible that both mechanisms are significant, the former coming into play on filling re-entrants, and the latter operative in straight sections of the die.

However, it is important to recognize the role of fraction solid and globule size in controlling the nature of such flow phenomena. Fig. 19 shows structures produced with a very fine globule powder (8 to 15  $\mu\text{m}$ ). Fig. 19a shows a cold pressed structure after brief heating into the semisolid region: it is noticeable that the molten magnesium-rich material has rapidly penetrated the fine interglobular spaces, despite the large disparity in size between the two powders, even without the assistance of pressure. After hot-pressing and die injection, the final microstructure is shown in Fig. 19b. It can be seen that globule depopulation near the casting surface is virtually absent, in contrast to products from coarser powders. The homogeneity of globule distribution in die-castings was quite striking for globule sizes below about 40  $\mu\text{m}$ . It is interesting to note that in this context that a comparably fine globule structure has never been generated by the rheocasting method.

Finally, Fig. 20 shows at low magnification a typical die-casting structure resulting when fibres were incorporated in the mixture. It was noticeable that the



*Figure 16* Structures from a mixture of two types of powder with alumina fibre. (a) Scanning electron micrograph of as-blended mixture, (b) scanning electron micrograph of billet 9, a cold-pressed blend after heating to the semisolid regime (but without hot pressing), and (c) optical micrograph of hot-pressed billet (billet 10).



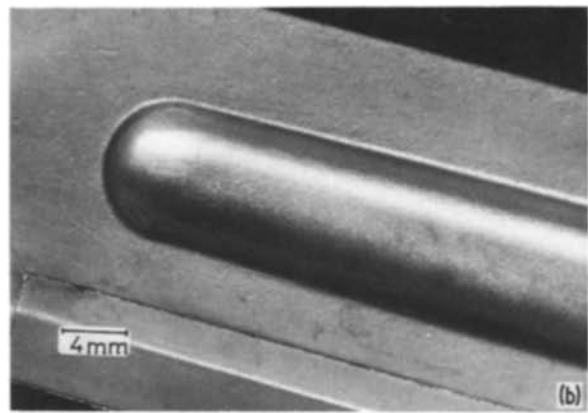
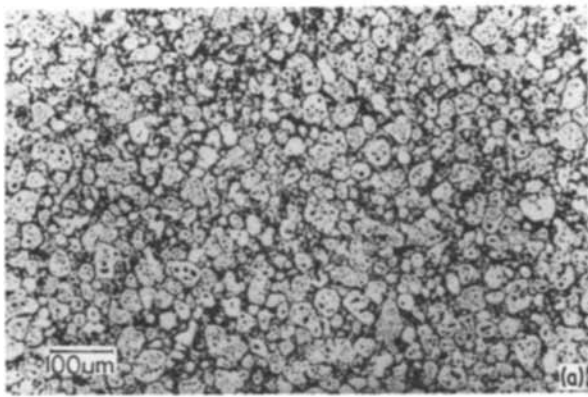


Figure 17 Typical appearance of die-castings. (a) Microstructure (billet 5) and (b) surface finish (billet 11).

overall distribution of fibres in the castings was surprisingly uniform (and randomly oriented) – indeed, it was consistently more homogeneous even than that in the hot-pressed billets. The only exception to this was an accumulation of fibre around the throat to the ingate area, which occurred in some castings. There were no obvious areas of fibre denudation. However, it must be noted that the fibre lengths were very short in these experiments (see Fig. 16b). It is not clear whether higher aspect ratio fibres in the charge (which could probably be produced by omitting the cold-pressing step) would become badly damaged during die injection and, if not, whether longer fibres would impede the fluid flow catastrophically or become inhomogeneously distributed in the casting. It is likely

that such problems will not prove insurmountable, and further work is needed in this area. In general, injection of slurries containing significant levels of fibre ( $\approx 10\%$  by volume) appears to require no special precautions other than a somewhat lower fraction of solid than would otherwise be used. Injection of material with higher fibre loadings than this has not yet been explored, but may well prove to be possible.

## 6. Discussion and conclusions

An indication has been given of how the processing of metals in the form of a semisolid slurry may confer advantages in terms of the ease, versatility and efficiency of fabrication, when compared with conventional solidification or deformation technology. These advantages are most effectively exploited if the slurry can be produced with a microstructure composed of globular (non-dendritic) solid suspended in a suitable liquid. The manufacture of such slurries has in the past been approached by dendrite fragmentation during solidification, most commonly via the continuous mechanical stimulation of localized shear. The techniques for doing this are subject to several limitations and the present article has explored certain features of an alternative method of producing suitable slurries, based on the mixing and heating of powders.

It has been shown that slurry microstructures can be tailored in a versatile fashion. Globule diameters ranging from 10 to 200  $\mu\text{m}$  have been generated and the volume fraction of solid can be accurately preselected over this range. Control of the fraction solid is important in view of its influence on the slurry viscosity (which must be regulated with precision if processing is to be successful). In the present case, this is determined by the temperature and by the extent of solute back-diffusion in the solid towards the globule centres. Investigation of this latter aspect has indicated a strong dependence on globule size, with neither the Scheil equation nor the lever rule universally applicable. In general, it has been found that appropriate selection of powder grades, compositions and consolidation conditions can lead to production of slurries with the desired microstructural features. These have, in turn, been used to produce die-castings with results which suggest that the technique may prove useful industrially. From these investigations, the following points have emerged.

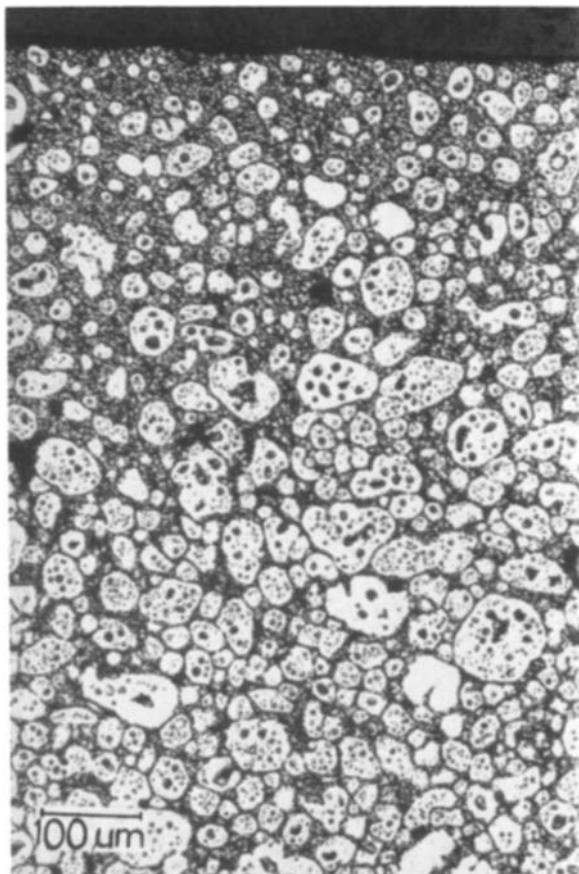


Figure 18 Optical micrograph of a section from a die-casting (from billet 7), showing the tendency for reduced globule populations to be generated near the casting surface.

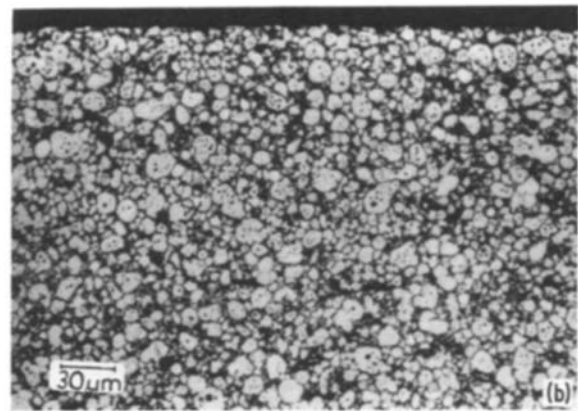
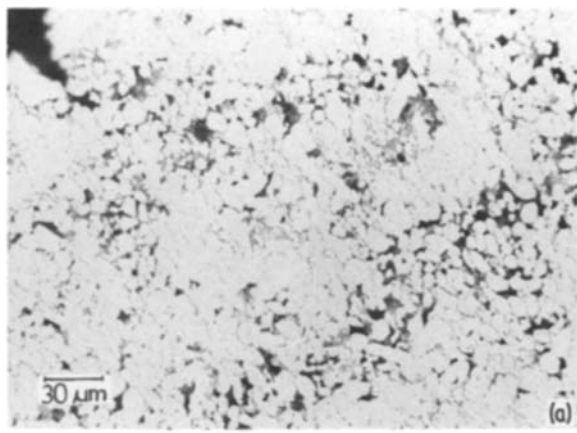


Figure 19 Structural development of a material containing very fine powder ( $\approx 8$  to  $15 \mu\text{m}$ ), (a) cold-pressed material after heating to the semisolid regime (billet 12), and (b) die-casting, near the surface (billet 13).

1. A relatively fine globule size ( $\approx 10$  to  $40 \mu\text{m}$  diameter) may be desirable for the following reasons:

(a) the system is then less prone to excessive transient melting as a result of slight overheating;

(b) the system rapidly approaches the condition dictated by the lever rule for the temperature concerned, allowing close control of the fraction of solid without the necessity of precisely programming the thermal history;

(c) there is a reduced incidence of globule depletion (and thus solute macrosegregation) in those regions of a die-casting prone to flow inhomogeneities. It may be that flow in constrained regions such as re-entrants and orifices is easier with smaller globules;

(d) if a ceramic dispersoid is incorporated in the original mixture, then its distribution tends to be more uniform and homogeneous.

2. The Scheil equation should not be used to predict the fraction solid at a given temperature in the semisolid regime (either during conventional rheocasting or for the present method of slurry production) unless the globule size is unusually coarse ( $\geq 200 \mu\text{m}$ ). In general, many cases will fall between Scheil and lever rule conditions and numerical computation is then necessary to explore the behaviour.

3. Coarsening rates are relatively slow, even with fine globules, and the structure changes little over the period corresponding to the minimum time in the semisolid regime for the route presented ( $\approx 10$  min).

4. The incorporation of ceramic fibres or other dispersoids can be achieved with little modification to the basic technique. Fibre damage was considerable, but this occurs during a cold pressing operation which is not considered to be an essential step in the process.

5. The incidence of microstructural or macrostructural defects can be low, both in the consolidated billet and in the finished die-casting. For example, the level of oxide in the products appeared from microstructural examination to be minimal.

6. The process can also be carried out with a single grade of alloy powder, although in this case the incidence of entrapped liquid appeared to be relatively high and this is expected to be undesirable.

7. The solute-enriched powder, which melts during processing, need not be very intimately mixed with, or be of a similar size to, the globule powder, as liquid infiltration of the globule array appears to take place very readily.

## Acknowledgements

The authors would like to thank Fulmer Research Laboratories and the SERC for financial support for one of us (RMKY) under the CASE award scheme. In addition, the considerable contribution of Dr G. B. Brook (the director of Research at Fulmer) to both theoretical and practical aspects of the work is gratefully acknowledged. Mr P. Caton and Mr N. Steward have been of great assistance during the die casting experiments at Fulmer.

## References

1. D. B. SPENCER, R. MEHRABIAN and M. C. FLEMINGS, *Met. Trans.* **3** (1972) 1925.
2. R. MEHRABIAN and M. C. FLEMINGS, *Trans. Amer. Foundryman Soc.* **80**(1972) 173.
3. M. C. FLEMINGS, R. G. RIEK and K. P. YOUNG, *Mat. Sci. Eng.* **25** (1976) 103.
4. D. G. BACKMAN, R. MEHRABIAN and M. C. FLEMINGS, *Met. Trans. B.* **8B** (1977) 471.
5. M. SUERY and M. C. FLEMINGS, *Metall. Trans. A* **13A** (1982) 1809.
6. B. SEYMOUR, L. E. SKINNER and G. H. WEST, *Metall. Mater. Technol.* (September) (1983) 445.
7. S. D. E. RAMATI, G. J. ABBASCHIAN, D. G. BACKMAN and R. MEHRABIAN, *Met. Trans. B.* **9B** (1978) 279.
8. L. LEHUY, J. MASOUNAVE and J. BLAIN, *J. Mater. Sci.* **20** (1985) 105.

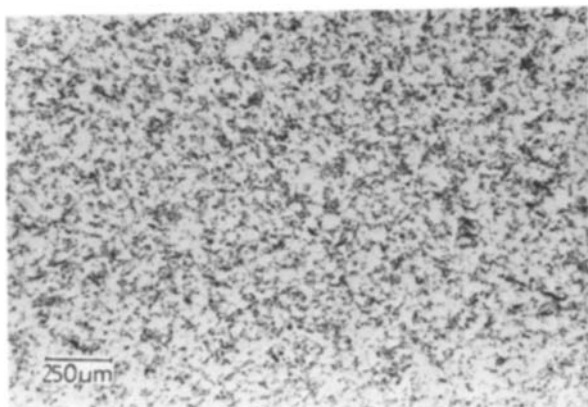


Figure 20 Typical microstructure of a die-casting containing fibre reinforcement (from billet 10).

9. G. B. BROOK, *Materials and Design*, **3** (1982) 558.
10. R. G. RIEK, A. VRACHNOS, K. P. YOUNG, N. MATSUMOTO and R. MEHRABIAN, *Trans. AFS* **83** (1975) 25.
11. M. YOSHIKAWA and T. ASAEDA, *Bull. JSME* **23** (1980) 476.
12. G. H. GEIGER and D. R. POIRER, "Transport Phenomena in Metallurgy" (Addison Wesley, Reading, Massachusetts, 1973) p. 31.
13. P. A. JOLY and R. MEHRABIAN, *J. Mater. Sci.* **11** (1976) 1393.
14. K. P. YOUNG, R. G. RIEK and M. C. FLEMINGS, in "Solidification and Casting of Metals" (The Metals Society, London, 1979) pp. 510-17.
15. M. C. FLEMINGS and R. MEHRABIAN, *Trans. AFS* **81** (1973) 81.
16. T. GILLESPIE, *J. Colloid Interface Sci.* **94** (1983) 166.
17. G. W. SWATZBECK and T. Z. KATTAMIS, *J. Mater. Sci.* **9** (1974) 635.
18. H. F. FISCHMEISTER and L. E. LARSSON, *Powder Metall.* **17** (1974) 227.
19. G. LANGFORD and D. APELIAN, *J. Metals* **23** (1980) 28.
20. B. C. PAI and H. JONES, in "Solidification Technology in the Foundry and Casthouse" (The Metals Society, London, 1983) pp. 126-300.
21. H. D. BRODY and M. C. FLEMINGS, *Trans. TMS AIME* **236** (1966) 615.
22. T. W. CLYNE and W. KURZ, *Met. Trans. A* **12A** (1981) 965.
23. V. LAXMANN and M. C. FLEMINGS, *ibid.* **11A** (1980) 1927.
24. A. VOGEL, *Metal Sci.* **12** (1978) 576.
25. C. J. SMITHELLS, "Metals Reference Book" (Butterworths, London, 1967) p. 675.
26. C. H. KANG and D. N. YOON, *Met. Trans. A* **12A** (1981) 65.
27. S. S. KIM and D. N. YOON, *Acta Metall.* **31** (1983) 1151.
28. P. W. VOORHEES and M. E. GLICKSMAN, *Met. Trans. A* **15A** (1984) 1081.
29. H. H. PARK, S. J. CHO and D. N. YOON, *ibid.* **15A** (1984) 1075.
30. T. H. COURTNEY, *ibid.* **15A** (1984) 1065.
31. K. TABESHFAR and G. A. CHADWICK, *Powder Metall.* **27** (1984) 19.
32. I. M. LIFSHITZ and V. V. SLYOZOV, *Phys. Chem. Sol.* **19** (1961) 35.
33. C. WAGNER, *Z. Electrochem.* **65** (1978) 489.
34. T. W. CLYNE, M. G. BADER, G. R. CAPPLEMAN and P. A. HUBERT, *J. Mater. Sci.* **20** (1985) 85.
35. M. C. FLEMINGS and G. E. NEREO, *Trans. TMS AIME* **239** (1967) 1449.
36. M. C. FLEMINGS, R. MEHRABIAN and G. E. NEREO, *ibid.* **242** (1968) 41.

*Received 23 April  
and accepted 5 June 1985*